CHAPTER 3

Material Preparation

&

Characterization Techniques

3.1 Introduction

This chapter contains several techniques to characterize the glass samples prepared using the "melt quench" technique. X-ray diffraction (XRD) was used to confirm that the samples were amorphous, which indicates that the glass was not crystalline in nature. This is an important characteristic of glasses, as it distinguishes them from other materials that have a defined crystal structure. Additionally, thermal characterization called TG-DTA to determine the glass transition temperature of the samples has been employed. This technique involves heating the sample and measuring the changes in mass and temperature as a function of time. The glass transition temperature is the temperature at which the glass transitions from a rigid, brittle state to a more flexible, rubbery state. A combination of experimental techniques has been used to fully characterize the glass samples using TG-DTA to determine the glass transition temperature.

Archimedes' principle was used to determine the density (ρ) of the prepared glass samples, wherein the acetone was used as a reference liquid with a density value of $0.784\ g/cc$. Density measurement is used to determine the mass of a substance per unit volume. It was used to calculate the molar volume (V_m), , which is the volume occupied by one mole of a substance, oxygen packing density (OPD) and total cation concentration (n_i). Fourier Transform Infrared (FTIR) spectroscopy is employed to study the vibrational modes of chemical bonds in a sample. By analyzing the characteristic frequencies of the vibrations, one can identify the types of chemical bonds present in the sample.

Impedance Spectroscopy/Complex Impedance Spectra (CIS) is used to study the electrical behaviour of a sample, specifically the ionic movement in glass electrolyte samples. By measuring the resistance and capacitance of the sample at different frequencies, one can analyze the conductivity, relaxation, dielectric and diffusivity of ions in the sample.

Furthermore, Scanning Electron Microscope (SEM) provides high-resolution images of the surface morphology of a sample. By using a focused beam of electrons to scan the sample, one can obtain detailed information about the surface structure and composition of the material. Fig. 3.1 depicts the conceptual framework for an entire experimental research tools carried out during the current study.

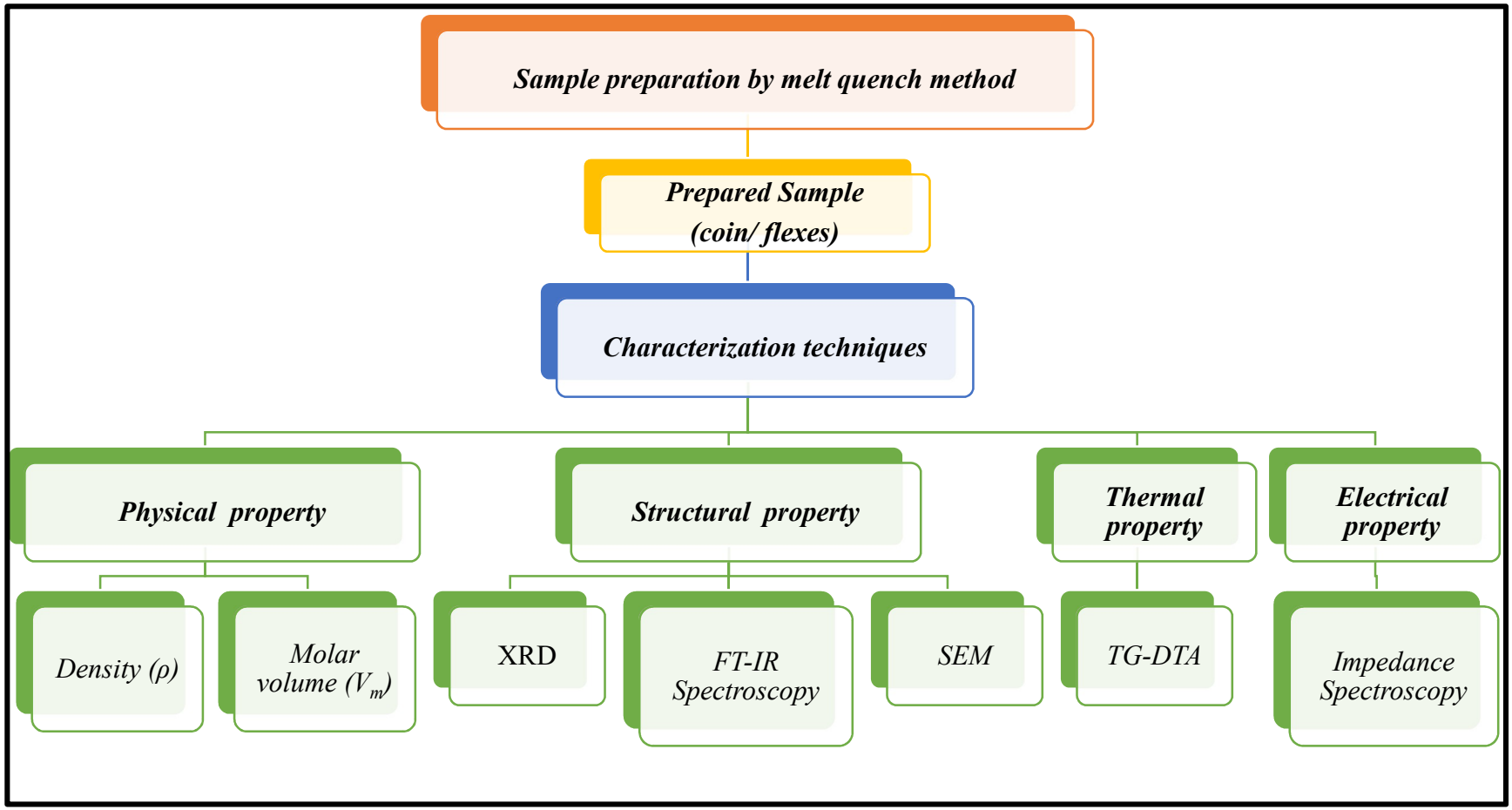

***Figure 3.1**:Experimental work-flow chart*

3.2 Method of Sample Preparation

The 'melt quench' by the rapid cooling process is one of the conventional and regularly used methods for preparing glass. The melt quench method is a popular method for synthesizing glass samples in laboratory and commercial purposes. In this method, the ingredients are mixed thoroughly and then melted at high temperatures before being quenched or cooled rapidly to form a glassy solid. The use of an electrical muffle furnace allows for precise temperature control and uniform heating of the mixture. Using analytical grade reagent chemicals and a micro analytical balance with an accuracy of $0.001\ mg$ ensures that the ingredients are weighed accurately and that the final product is of high purity. Mixing the ingredients thoroughly with an agate mortar and pestle ensures that the ingredients are evenly distributed, which is important for the final properties of the glass. Using a quartz crucible is preferred for its high resistance to thermal shock and chemical corrosion. Heating the mixture in an electrical muffle furnace provides precise temperature control, which is important for obtaining the desired properties of the glass as shown by Fig. 3.2.

The furnace has two main components: the heating element, which is made of Super Canthal wire, and the control unit, which regulates the temperature of the furnace using an E-M relay.

***Figure 3.2**: Electric muffle furnace*

To measure the temperature, the furnace uses Chromel-Alumel (Type K) wired thermocouples, which can measure a wide temperature range from $(30℃ - 1200℃)$ with a normal precision of $\pm 1℃$. Before using the furnace, it's common practice to heat it up to a specific temperature to remove any water or other impurities from the furnace. Hence, the furnace was heated to $500℃$ and held at that temperature for half an hour to remove any H_2O and CO_2 from the mixture.

The process for producing glass samples through melting, stirring, and rapid cooling, the temperature range from 800℃ to 1050 ℃ and duration of heating was maintained for 8 − 10 hours for preparing the glass samples. After the glass has been melted and stirred to ensure a homogeneous mixture, it is rapidly cooled by pouring it between two copper blocks. This rapid cooling process is known as quenching and helps to prevent crystal formation within the glass. As a result, the coin/flex-like shaped glass samples were obtained and placed in a preheated furnace. Once the glass samples have been quenched, they may still contain residual thermal stresses. To remove these stresses, the samples are placed in a preheated furnace at a temperature of 150℃ to 200℃ for two hours. This process, known as annealing, helps to relax the internal stresses in the glass and prevent cracking or other damage when the glass is used in further experiments.

To investigate the mechanism of conductivity and relaxation in borophosphate glass system, the following three sets of glass samples were prepared.

Series (a): $x(LiI)$: $\{(100-x)[60\ Li_2O:(8\ B_2O_3+32\ P_2O_5)]\}$, known as LBP

$$where, 0 \leq x \leq 25\ wt.\%, with\ interval\ of\ 5\ unit$$

Series (b): $x(NaI)$: $\{(100-x)[30Na_2O:(56\ B_2O_3+14\ P_2O_5)]\}$, known as NBP

$$where, x = 1, 2.5, 4, 5, 10, 15, 20\ wt.\%$$

Series (c): $x(AgI)$: $\{(100-x)[30\ Ag_2O:(56B_2O_3-14\ P_2O_5)]\}$, known as ABP

$$where, x = 0, 1, 3, 5, 7\ wt.\%$$

Here, in all the glass series, the impact of varying amounts of metal iodide salt on the different physical properties of host metal oxide-modified borophosphate glass has been studied.

3.3 Experimental Techniques:

After the preparation of the samples, to ascertain their fundamental nature and properties, characterization studies were conducted.

3.3.1 Physical Characterization:

Density (ρ) is a fundamental physical property of all substances, and it is defined as the amount of mass per unit volume of a material. Archimedes' principle has been a commonly used method for determining the density of an object. It states that the buoyant force on an object submerged in a fluid is equal to the weight of the fluid displaced by the object.

By measuring the weight of an object in air and in water, the volume of the displaced water can be calculated, and hence the density of the object can be determined using the formula: $density = {Mass}/{Volume}$; where mass is the mass of the object and volume is the volume of the displaced water. This principle is particularly useful for measuring the density of irregularly shaped objects or substances that are difficult to measure by other means. The reference immersing liquid is acetone of a known density value of 0.784 g/cc, which was employed to calculate density. Bulk glass flex was weighed in the air using a micro digital balance, and then weighed again after being immersed in acetone (Fig. 3.3). Therefore, the weight difference between the bulk glass flex in air and when immersed in acetone is equal to the weight of the acetone displaced by the bulk glass flex. The density was determined using measured data using the following Eq. (3.1).

***Figure 3.3**: Density of Glass sample using Archimedes Principle.*

$$\rho_{sample} = \rho_{liquid}\, x \left[\frac{M_{air}}{M_{air} - M_{liquid}}\right] g/cc \quad \ldots\ldots (3.1)$$

where, ρ_{sample} is the density of a specimen, ρ_{liquid} is the reference liquid density (Acetone: 0.784 g/cc), M_{air} is the mass of the sample in air, and M_{liquid} is the mass of the sample in liquid (acetone).By using density, the molar volume of the multi-component glass system has been determined by using Eq. 3.2. By computing the molar volume, one mole of oxygen can be re-defined. Until the glass network expands, the empty sites in the glass network are too small to hold modifier ions with high polarizability and a large ion radius.

$$V_m = \frac{\bar{M}}{\rho} = \frac{Average\ molecuar\ weight}{Density}\ (cc/mole) \quad \ldots\ldots (3.2)$$

"This study investigates the compositional dependency of the density and molar volume of metal iodide-doped and metal oxide-modified borophosphate glasses as a function of varying concentrations of metal iodide in the host glass matrix".

3.3.2 Structural Characterization:

a) X-ray Powder Diffraction (XRD)

X-ray diffraction (XRD) is a powerful analytical technique used to investigate the structure of materials on an atomic and molecular level. In this study, X-ray beam falls onto a sample, which then diffracts (bends) the X-rays in specific patterns that can be measured and analyzed to reveal information about the arrangement of atoms or molecules in the sample. X-ray powder diffraction is particularly useful for analyzing crystalline materials, as the repeating structure of the crystals produces distinctive diffraction patterns that can be used to identify the crystal structure and other properties of the material.

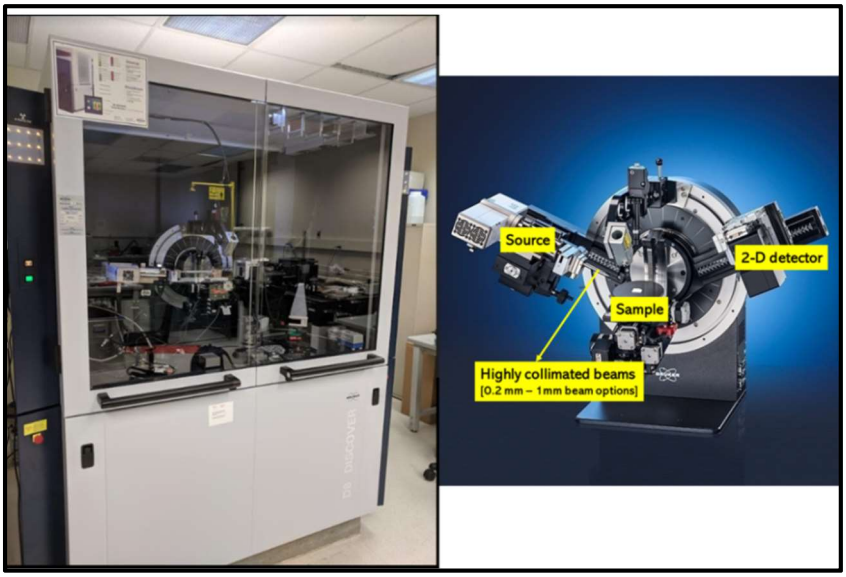

***Figure 3.4**: Bruker Discovery-D8 X-ray diffractometer.*

One advantage of XRD is that it can be used to analyze materials without destroying or significantly altering the sample. X-ray diffraction (XRD) is used to investigate the structure of materials, including glasses, metals, fluids, ceramics, semiconductors, and thin films. X-rays have wavelengths that are similar to the interatomic distances in crystals, making them well-suited for studying the arrangement of atoms in crystalline materials.

In addition to studying crystalline materials, XRD can also be used to investigate the structure by analyzing the diffuse scattering of X-rays from an amorphous material, and can gain insights into the short-range order and structure of the material. The X-ray pattern shows how the atoms are arranged in a crystal. Amorphous substances, like glass, lack a periodic array with long-range order; hence, they do not generate a diffraction pattern. As the inter-planar spacing in a crystal is typically of the order of several angstroms (Å), the

atomic planes can diffract electromagnetic radiation such as X- rays with wavelengths equivalent to the inter-planar spacing. If the Bragg condition (Eq. 3.3) is satisfied, a monochromatic X-ray beam will diffract.

$$n\lambda = 2d \sin\theta \quad \ldots\ldots (3.3)$$

where λ is the X-ray wavelength, d is the inter-planar spacing, θ is the glancing angle between the incident beam and the scattering atomic planes, and n is an integer that indicates the order of diffraction.

Practically, the angle of diffraction is typically given as 2θ rather thanθ. In amorphous materials, such as glasses and liquids, there is no long-range periodic structure; hence, Bragg's law is utterly irrelevant. Amorphous materials, unlike crystals, do not create X-ray or electron diffraction patterns with strong Bragg peaks.

Instead, distinctive diffused and broad humps are observed. In the present study, a Bruker Discovery diffractometer-D8 (Fig. 3.4) was utilised to examine and record the X-ray diffraction patterns at room temperature for the prepared bulk glass samples (in finely powdered form) using monochromatic $Cu - K\alpha$ radiation as a source with a wavelength of $\lambda = 1.5418$ Å. The diffraction spectra were recorded for 2θ, which varied from 10^0 to 80^0 at a rate of $2^0/\text{minute}$ (slow scan).

b) FT-IR Spectroscopy

Fourier Transform Infrared Spectroscopy (FTIR) is a widely used analytical technique that provides information about the molecular structure of a sample. FTIR measures the absorption or transmission of infrared radiation as a function of frequency or wave length. When IR radiation passes through a sample, certain frequencies of the radiation are absorbed by the sample, while others are transmitted. The absorbed frequencies correspond to the vibrational frequencies of the chemical bonds in the sample. FTIR measures the absorption of infrared radiation over a wide range of frequencies simultaneously, which allows for the identification of a large number of different functional groups and chemical bonds in a sample. The positions and shapes of the peaks in the spectrum correspond to the different types of chemical bonds present in the sample, which can be used to identify the sample's composition and structure. Comparing the FTIR spectrum of an unknown sample to those of known standards can help to identify the specific functional groups and chemical bonds present in the sample. In IR spectroscopic analysis, the main objective is to identify the chemical functional groups present in a sample. The IR range of the electromagnetic

spectrum typically spans from 4000 to 400 cm^{-1}. The wave number (n) represents the number of waves per unit length and is often used to quantify the position of IR absorption peaks. In modern IR spectroscopy, Fourier Transform Infrared (FT-IR) spectroscopy is widely used. FT-IR spectra are commonly represented as the percentage of light transmittance or absorbance plotted against the wave number (cm^{-1}), which is the reciprocal of the wavelength.

By analyzing the IR spectra of a sample, it is possible to determine the characteristic absorption bands corresponding to specific functional groups. This allows for the identification and characterization of various chemical bonds and molecular structures present in the sample. IR spectroscopy is a valuable tool in organic and inorganic chemistry, as well as in various other scientific fields.

On the other hand, the wavelength is inversely related to the frequency and the energy that goes with it.

$$\bar{\nu}(cm^{-1}) = \frac{1}{\lambda\ (\mu m)} x\ 10^4 \quad \ldots\ldots (3.4)$$

Fourier Transform Infrared (FT-IR) system works by measuring the intensity of IR radiation that passes through or reflects off a sample over a range of frequencies. FT-IR spectrometers use an interferometer to generate an interferogram, which contains information about the intensity of the IR radiation as a function of the path difference between two beams of IR light. This interferogram is then transformed using Fourier analysis to obtain the spectrum of the sample.

The spectrum obtained in FT-IR spectroscopy is typically plotted as a graph of intensity (y-axis) versus wave number (x-axis), where wave number is the reciprocal of wavelength and is measured in units of cm^{-1}. In transmission mode, the spectrum shows troughs, or areas of decreased intensity, at the frequencies where the sample absorbs IR radiation. The positions and intensities of the peaks or troughs in the IR spectrum provide information about the molecular vibrations present in the sample. This information is used to identify the sample and to study its chemical structure and properties. At temperatures above absolute zero, all atoms in molecules vibrate continuously about one another. In resonant conditions, when the frequency of their vibrations is the same as the frequency of IR, radiation is absorbed by the molecules, and then re-emit. Each atom has the freedom to move along the three Cartesian coordinate axes (x, y, z), called "degrees of freedom".

Polyatomic molecules with $'n'$ atoms have a total of $'3n'$ degrees of freedom that describe the translation of the molecule are the movement of the molecule along the $x, y,$ and z axes. The three other motions related to the rotation of the whole molecule are the rotation about the $x, y,$ and z axes. The remaining $'3n-6'$ degrees of freedom are the normal modes of vibration, which refer to the oscillation of the atoms within the molecule. These vibrations can occur in three different ways: stretching (where the bond length changes), bending (where the bond angle changes), and twisting (where the dihedral angle changes). When a molecule absorbs infrared radiation, it causes these normal modes of vibration to be excited. The frequency and intensity of absorption bands observed in the IR spectrum are unique to each compound and provide valuable information about the functional groups present in the molecule. The mixing and blending of coupling interactions and overtones can complicate the IR spectrum, but it can also provide additional information about the molecule's structure and composition.

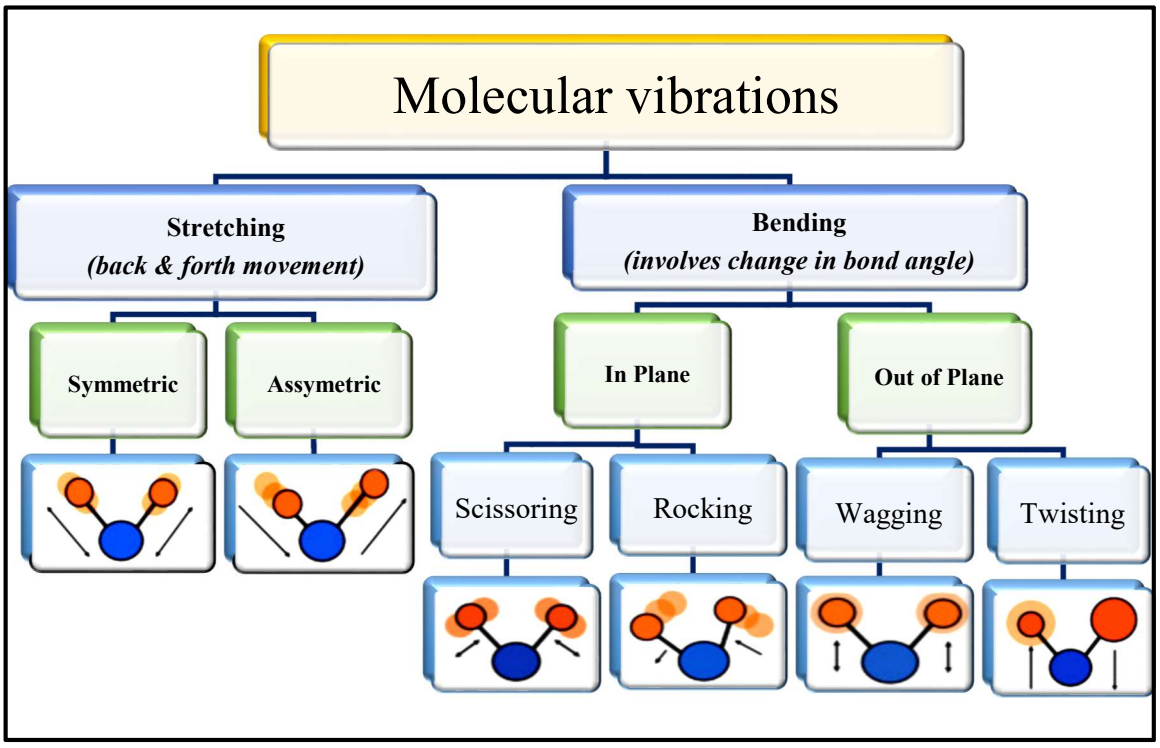

***Figure 3.5**: Characteristic vibrational modes of chemical bond.*

Out of all of these, stretching and bending are the predominant vibrations. Fig. 3.5 depicts the different kinds of vibration movement of non-linear tri-atomic water molecules. When the molecules absorb IR radiation, the radiation energy is transferred to them, leading to various molecular behaviours.

The individual vibrational motion of a molecule is typically accompanied by rotating motion, resulting in an absorption band rather than discrete lines in the mid-infrared region. There are three fundamental spectrometer components in the Fourier transform system: a radiation source, an interferometer, and a detector. Fig. 3.6 (a-b) depicts the block diagram and a typical FT-IR spectrometer. The intensity of transmitted or reflected light at each wavelength is measured using a detector. The resulting signal from a detector machine is then evaluated on a computer using Fourier Transform to generate the FT-IR spectrum for study. Most of the time, the FT-IR output spectrum shows the amount of light transmitted or absorbed as a function of the wavenumber (reciprocal of wavelength in cm^{-1}).

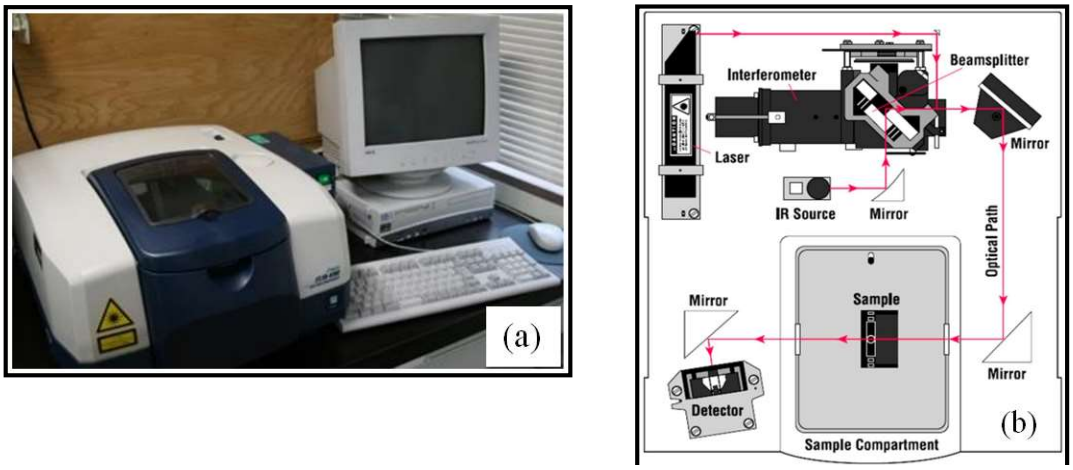

Figure 3.6: *(a) FT-IR spectrometer-JASCO model 4000 image, (b) Block diagram of typical FT-IR Spectrometer.*

In this work, the FT-IR spectrometer JASCO FTIR was used to study the structural units of LBP, NBP, and ABP glass systems in the wave number range of $400-4000\ cm^{-1}$ (with a standard resolution) at room temperature. IR grade quality dry potassium bromide (KBr) powder ($100\ mg$) and a small amount of the powdered sample (1 to $2\ mg$) were mixed, ground, and then compressed to make a pellet of $0.5-1\ mm$ thickness.

3.3.3 Thermal Characterization:

Thermal analysis is a set of techniques used to study the thermal properties and can be used to investigate a wide range of materials, from polymers and plastics to glasses. Differential Scanning Calorimetry (DSC) is one of the most commonly used thermal analysis techniques. It measures the difference in heat flow between a sample and a reference material as the temperature is varied, and it can be used to determine a wide range of thermal properties, including the melting temperature (T_m), glass transition temperature (T_g), heat of fusion, and heat capacity and crystallisation temperature (T_c).

Thermo-gravimetric analysis (TGA) measures the change in mass of a sample as a function of temperature or time, and it can be used to determine the thermal stability, decomposition temperature, and other properties of materials, while Differential thermal analysis (DTA) measures the temperature difference between a sample and a reference material as the temperature is varied, and it can be used to detect phase transitions, melting points, and other thermal events. When combined in a single instrument, TGA-DTA can provide a more complete picture of the thermal behavior of a material, allowing researchers to study both mass loss and temperature-related changes in properties such as crystallinity, phase transitions, and chemical reactions.

The present study was done with TG-DTA thermal analyser, with a focus on the DTA technique using the model NETZSCH-STA-449 F3 and its block diagram, Fig. 3.7 (a-b), for thermal analysis. It helps measure the flow of heat (mW/mg) in materials as a function of time and temperature.

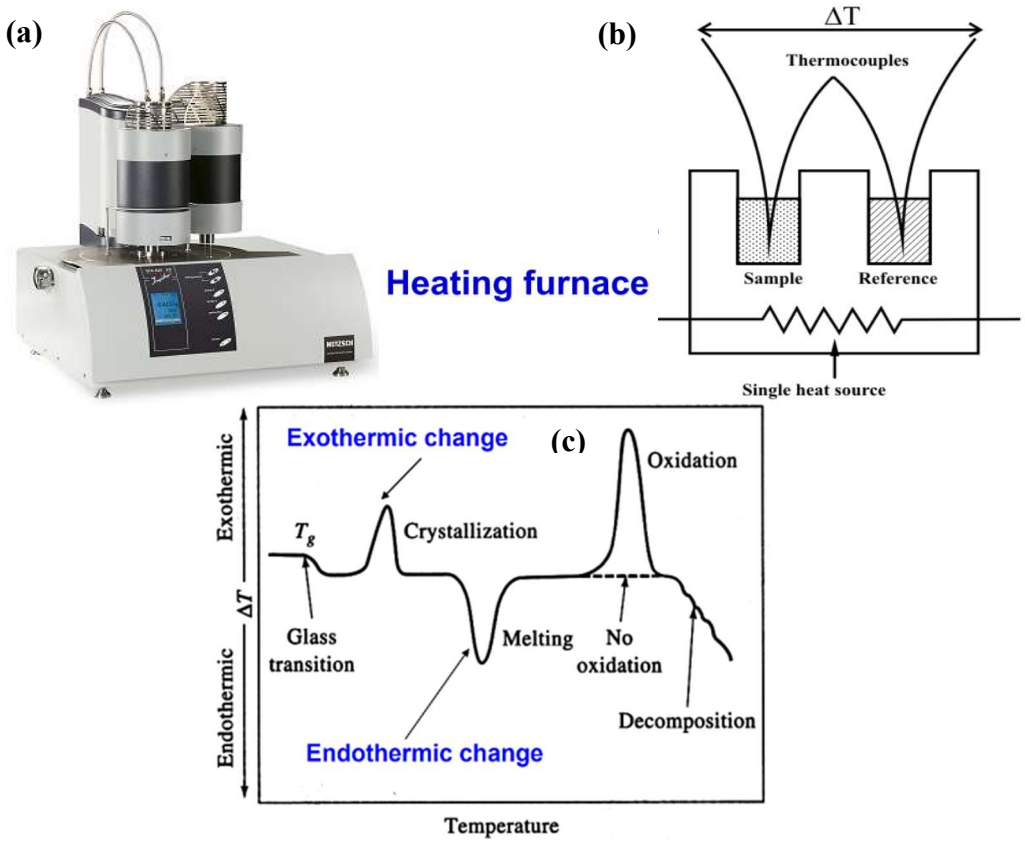

Figure 3.7: (a) NETZSCH STA 449 F3– Thermal Analysis System, (b) block diagram of DTA thermal analyser, (c) a typical DTA thermogram.

These measurements give both quantitative and qualitative information about physical and chemical changes that are endothermic (absorption of energy) or exothermic (liberation of energy), or involve changes in heat capacity / glass transition.

The difference in heat flow between the sample and the reference is represented on the Y-axis of the DTA plot, while X-axis denotes temperature. The heat, q, supplied per unit time, t, represents the heat flow. Temperature increases ΔT per unit of time, t, is the heating rate.

$$Heat\ flow = \frac{heat}{time} = \frac{q}{t} \quad \ldots\ldots (3.5), and\ Heating\ rate = \frac{\Delta T}{t} \quad \ldots\ldots (3.6)$$

$$\therefore Heat\ capacity = C_p = \frac{q/t}{\Delta T/t} = \frac{q}{\Delta T} \quad \ldots\ldots (3.7)$$

The heat capacity (C_p) of a substance is the amount of heat required to raise its specific temperature. Initially, at a specific temperature point shown in the Fig. 3.7(c), the horizontal line on a DTA thermograph suddenly moves down from its baseline. It shows that the sample absorbs heat and increases its heat capacity but not involving the phase transition, which appears as the glass transition temperature (T_g).

In the investigation, the analysis of amorphous materials was carried out using the Differential Thermal Analysis (DTA) technique with a NETZSCH STA 449 F3 thermal analyzer. This analysis aimed to confirm the amorphous nature of the materials and determine their glass transition temperature. DTA is a thermal analysis technique that measures the temperature difference between the sample and a reference material as a function of temperature. By subjecting the sample to a controlled temperature program, it allows for the detection of thermal events such as phase transitions, crystallization, and melting. In the DTA analysis, an Al_2O_3 crucible was used to hold the sample. The temperature range of the analysis was set between 27℃ and 1000℃. The analysis was conducted in an inert environment of nitrogen (N_2) to prevent any unwanted reactions or oxidation of the sample. By performing DTA analysis, the glass transition temperature of the amorphous materials under investigation could be determined. The glass transition temperature is the temperature at which the amorphous material transitions from a rigid, glassy state to a more mobile and rubbery state. This transition is accompanied by a slight shift in the DTA peak, indicating the absorption of latent heat while the heat capacity of the material increases.

The DTA analysis provided valuable information about the thermal behavior of the amorphous materials, confirming their glassy nature and determining their glass transition temperature. This data is important for understanding the thermal properties and behavior of these materials, which is crucial in various applications and material characterization studies.

3.3.4 Scanning Electron Microscope (SEM):

Scanning Electron Microscopy (SEM) is a tool for imaging and analyzing the surface of solid specimens. In SEM, Fig. 3.8(a), a focused beam of high-energy electrons is raster-scanned over the specimen, and the interaction of the electrons with the sample generates a variety of signals, including secondary electrons, backscattered electrons, and characteristic X-rays. These signals are then detected and processed to form an image of the specimen's surface. SEM can provide high-resolution images with a magnification range from a few tens of times to more than a million times. SEM can reveal details of the surface morphology, crystal structure, elemental composition, and chemical bonding of a sample, making it a valuable tool for both qualitative and quantitative analysis. The block diagram of key components is shown in the Fig. 3.8 (b).

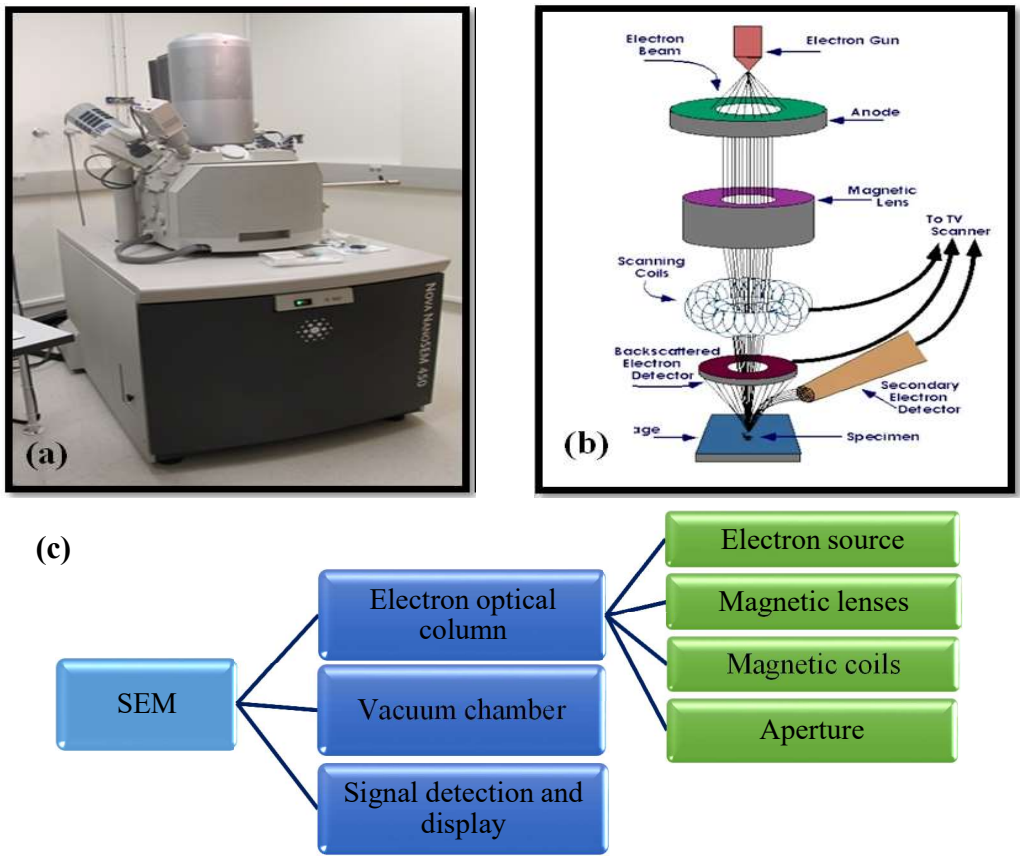

Figure 3.8: *(a) Field Emission Gun Nano Nova Scanning Electron Microscope (FEG-SEM) 450, (b) Block diagram of typical SEM, (c) Key components of SEM machine.*

The SEM consists of three primary components: the electron source, the electron optics, and the vacuum system. The electron source, typically a heated tungsten filament or a field-emission gun, generates a beam of high-energy electrons. These electrons are then focused and controlled by a series of electromagnetic lenses and apertures in the electron optics column, which is typically made up of magnetic coils and electrostatic lenses. The magnetic

coils are used to control the direction and intensity of the electron beam, while the apertures help to shape and focus the beam. The vacuum system is another critical component of the SEM. Since the electron beam can be easily scattered and absorbed by air molecules, a high vacuum environment is necessary for the SEM to function properly. The vacuum chamber creates and maintains a vacuum, typically in the range of 10^{-3} to 10^{-7} torr, by removing air and other gases from the sample chamber. Overall, these components work together to generate an electron beam, control its trajectory and focus, and detect the signals emitted by the sample, which are then processed to produce an image. In the present study, surface characteristics/ topography (how it looks) of an object that correlates with its material attributes.

3.3.5 Electrochemical Impedance Spectroscopy Analysis:

AC impedance spectroscopy is a widely used technique in electrochemistry and materials science for characterizing the electrical properties of materials, including solid electrolytes. The technique involves applying a small-amplitude sinusoidal current to the sample and measuring the resulting voltage response. By analyzing the complex impedance of the sample as a function of frequency, various electrical properties such as resistance, capacitance, and conductivity can be determined. In the case of solid electrolyte samples, impedance spectroscopy can be used to determine the electrical conductivity using Eq. 3.8, which is only valid if the bulk impedance of the electrolyte sample is known. This is because at the electrolyte/electrode interface, the uni-directional DC flow of current creates a polarisation cloud, which creates a concentration gradient inside the electrolyte, and eventually ionic current value drops to zero. This phenomenon is known as electrode polarization and can lead to an overestimation of the electrolyte conductivity if not properly accounted for. To overcome this issue, various correction methods can be employed, such as applying a small AC bias to the DC measurement to separate the bulk and interfacial impedance contributions.

$$\sigma = \frac{t}{zA} \quad \ldots\ldots (3.8)$$

Where, σ is conductivity, t is the thickness of the sample, z is the impedance and A is the cross sectional area of the sample.

When a direct current (DC) is applied to an ionic conductor, the accumulation of charge at the electrodes can create a space charge region, which can impede the flow of ions and electrons through the material. This can result in inaccurate measurements of the material's ionic conductivity. On the other hand, using an alternating current (AC) field can help to

mitigate the effects of space charge development and ion/electron charge transfer at the electrodes. The changing polarity of the AC field can effectively cancel out any net charge accumulation, allowing for more accurate measurement of the material's bulk conductivity. In addition, AC methods can also provide additional information about the material's frequency-dependent behaviour, which can be useful in characterizing the underlying mechanisms of ion conduction in the material.

In AC impedance measurements, a small sinusoidal signal is applied to the sample over a range of frequencies, and the response of the sample is measured. The response is typically characterized by two parameters: the magnitude of the impedance (or its reciprocal, the admittance) and the phase angle between the applied signal and the response. The magnitude of the impedance is related to the resistance and capacitance of the sample, while the phase angle reflects the time delay between the applied signal and the sample's response. By analyzing the magnitude and phase angle as a function of frequency, information about the sample's electrical properties can be obtained. In the case of ionic solids, solid electrolytes, ion-conducting glass and polymer structures, the AC impedance measurements can reveal information about the diffusion mechanism of the ions or molecules through the material. The phase angle can indicate the time delay between the applied signal and the diffusion process, while the magnitude of the impedance can provide information about the resistance of the material to the diffusion process.

Formalisms of impedance spectroscopy:

The complex plane analysis of electrical parameters is a mathematical technique that involves both the real and imaginary parts of complex electrical quantities. Complex electrical quantities, such as impedance, admittance, permittivity, and modulus, are interrelated and arise from the same microscopic events. However, each of these parameters contributes uniquely to the ion conduction mechanism. For instance, the complex impedance (Z^*) describes the opposition to the flow of an alternating current, whereas the complex admittance (Y^*) represents the ease with which an alternating current flows through a circuit. On the other hand, the complex permittivity (ε^*) characterises the ability of a material to store electrical energy in an electric field , while the complex modulus (M^*) represents the resistance of a material to deformation under applied stress or force. The subsequent chapter will discuss each of these in turn. The Table 3.1 provides a concise summary of the relationship between these parameters.

***Table 3.1**: Various formalisms of impedance spectroscopy and their interrelationships with complex impedance.*

Electrical parameter	Mathematical Expression $f(\omega)$	Real & Imaginary part
Impedance (Z^*)	$Z^* = Z' - iZ''$ $Z^* = \|Z\|e^{-i\omega t}$ $Z^* = \|Z\|\ (cos\omega t - i\ sin\omega t)$	$Z' = \|Z\|\ cos\varphi$ $Z'' = \|Z\|\ sin\varphi$
Admittance (Y^*)	$Y^* = Y' + iY''$ $= \frac{1}{Z^*}$ $= \frac{1}{Z' + iZ''}$	$Y' = \left(\frac{Z'}{Z'^2 + Z''^2}\right)$ $Y'' = \left(\frac{Z''}{Z'^2 + Z''^2}\right)$
AC conductivity	$\sigma^* = \sigma' + i\sigma''$ $\sigma^* = \frac{t}{a}\left(\frac{Z' + iZ''}{Z'^2 + Z''^2}\right)$	$\sigma' = \frac{t}{a}\left(\frac{Z'}{Z'^2 + Z''^2}\right)$ $\sigma'' = \frac{t}{a}\left(\frac{Z''}{Z'^2 + Z''^2}\right)$
Dielectric Permittivity (ε^*)	$\varepsilon^* = \varepsilon' - i\varepsilon''$ $\varepsilon^* = \frac{1}{i\omega C_0}Y^*$ $\varepsilon^* = \frac{1}{i\omega C_0}\frac{1}{Z^*}$	$\varepsilon' = \frac{-i}{\omega C_0}\left(\frac{Z''}{Z'^2 + Z''^2}\right)$ $\varepsilon'' = \frac{-i}{\omega C_0}\left(\frac{Z'}{Z'^2 + Z''^2}\right)$
Modulus (M^*)	$M^* = M' + iM^{"}$ $M^* = \frac{1}{\varepsilon^*}$ $M^* = i\omega C_0 Z^*$ $M^* = i\omega C_0(Z' - iZ'')$	$M' = \omega C_0 Z''$ $M'' = \omega C_0 Z'$

where,

$\omega = frequency = 2\pi f$

$\varphi = arc\ tan(Z"/Z') = phase\ diff.\ between\ applied\ potential\ and\ response\ current$

$|Z| = \sqrt{Z'^2 + Z''^2}$

$t =\ thickness\ of\ the\ sample(mm)$

$a =\ cross\ section\ area\ of\ the\ sample(mm)^2$

$\varepsilon_0 = Free\ space\ permittivity = 8.85x10^{-12}F/m$

$C_0 = capacitance\ (geometric) of\ the\ electodes = \varepsilon_0\ (a/t)$

In 1969, Baurale was the first to use impedance spectroscopy to study the response of zirconia solid electrolyte cells to sinusoidal disturbance. Since then, the technique has been widely used to study a variety of materials. In the AC method of impedance spectroscopy, a small AC signal is applied to the sample, and the resulting current is measured. By comparing the magnitude and phase shift of the output signal at a given frequency to the input-reference signal, one can calculate the impedance of the material. This allows to study the electrical properties of the material over a wide range of frequencies and temperatures. The function of the applied sinusoidal voltage can be written as shown in Eq. (3.9).

$$V_{(t)} = V_m e^{i\omega t} \quad \ldots\ldots (3.9)$$

Then the AC current corresponding to this potential can be expressed as follows.

$$I_{(t)} = I_m e^{(i\omega t+\varphi)} \quad \ldots\ldots (3.10)$$

(a) Complex Impedance Formalism

Impedance is a measure of the opposition that a circuit element presents to the flow of an alternating current. It is a complex quantity that includes both a real component (Z') and an imaginary component (Z''), and is often expressed in polar form as $\boldsymbol{Z} = |\boldsymbol{Z}|\angle\varphi$, where $|\boldsymbol{Z}|$ is the magnitude of the impedance and φ is its phase angle. Nyquist plots are graphical representations of complex impedance or transfer functions, as shown in Fig. 3.9. They display the real part of the impedance (Z') on the x-axis and the imaginary part (Z'') multiplied by (-1) on the y-axis. The resulting plot shows the frequency response of the system, with the magnitude of the impedance represented by the distance from the origin and the phase angle represented by the angle of the line connecting the origin to the point on the plot. Typically, the Nyquist plot for glassy electrolyte materials resembles the illustration mentioned in Fig. 3.9.

A modest signal ac test on such a cell reveals that its impedance is often frequency-dependent and can be described by a network of resistances and capacitance known as an 'equivalent circuit'. In the Nyquist plots, Fig. 3.9, of electrochemical impedance spectroscopy data, each point represents the impedance at a particular frequency, with low-frequency data on the right and high-frequency data on the left.

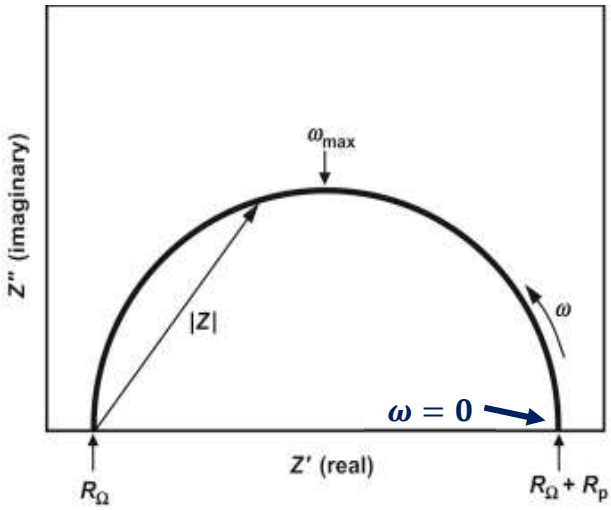

***Figure 3.9**: Nyquist plot of a typical electrochemical system.*

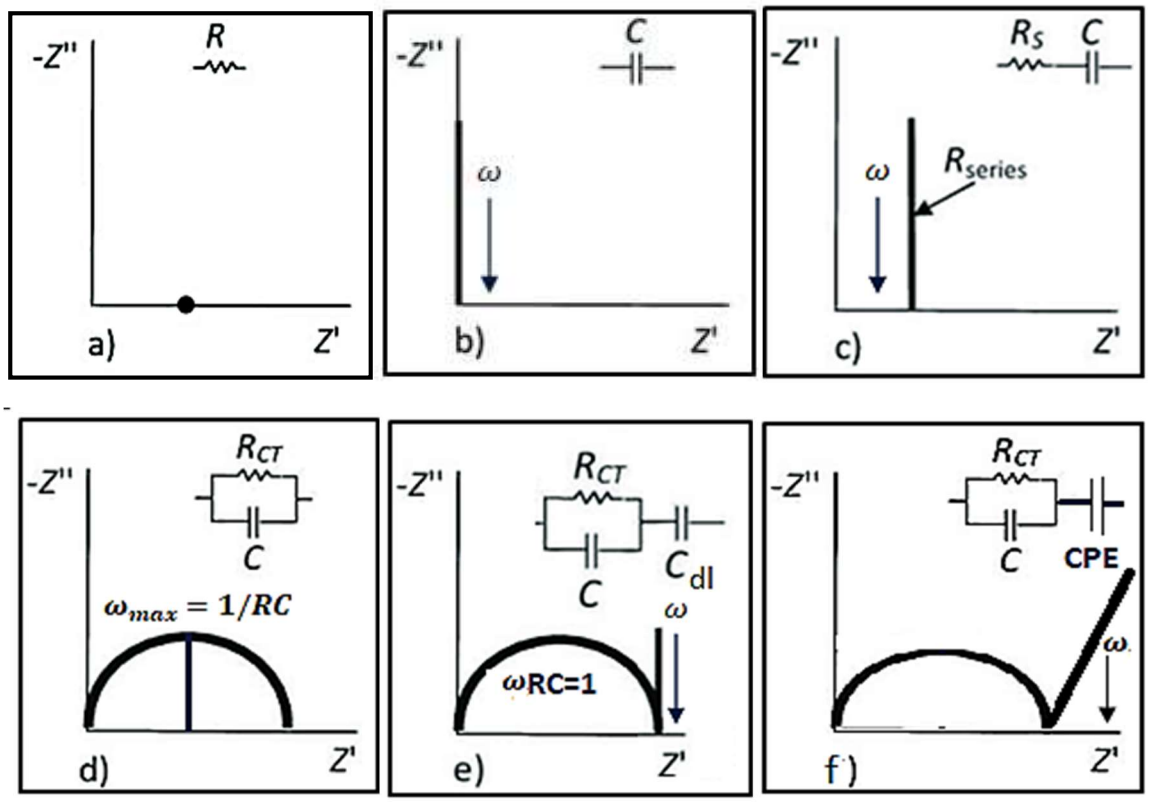

***Figure 3.10**: Impedance spectra for (a) pure **R**, (b) pure **C**, (c) **RC** series, (d) **R ll C**, (e) **R ll C** with blocking electrode (ideal), (f) **R ll C** with leaky CPE element (real).*

It is possible to evaluate disordered electrolyte systems in terms of resistive behaviour brought on by ion mobility and capacitive behaviour resulting from lattice polarisation. Therefore, it is essential to describe the type of behaviour expected from pure R, C and their probable combinations to characterize the complex impedance plots of the investigated material. Fig. 3.10(a) shows the impedance of a pure resistance R, which is equal to its

resistance value R. This impedance is independent of frequency and corresponds to a vector terminating at the point R on the real axis of the complex impedance plane. On the other hand, the impedance of a pure capacitance C is given by $Z = (-i2\pi fC)^{-1}$, which depends on the inverse of frequency (f^{-1}). As the frequency increases, the impedance of the capacitor decreases, approaching zero as the frequency becomes infinite. In the complex impedance plane, each measured frequency corresponds to a point on the imaginary axis. The lower the frequency, the higher the impedance, and the closer the point is to the vertical axis. As the frequency increases, the impedance decreases, and the point moves down towards the origin. The infinite frequency points for all passive components form a straight line on the imaginary axis, which is known as the "asymptote" or "tail" of the impedance curve Fig. 3.10(b)**.** As shown in the Fig. 3.10(c), a series combination of resistance R and a capacitance (C) exhibits a line parallel to the imaginary axis and an intersection on the real axis at R $(Z' = R)$ in the complex plane of the impedance plot.

The impedance of a parallel combination of resistance (R) and capacitance (C) can be expressed as Eq. 3.11, where $'i'$ is the imaginary unit, and ω is the angular frequency of the AC signal applied to the circuit. In this expression, the real part of the impedance is Z', which corresponds to the intersection of the semicircle with the real axis at R is given by Eqs. 3.12 and 3.13. The imaginary part of the impedance Z'' is given by Eq. 3.14, which corresponds to the vertical distance between the semicircle and the real axis at a given frequency.

As illustrated in the Fig. 3.10(d), a parallel combination of resistance R and capacitance C results in a semicircle $\left[\left(Z' - \frac{R}{2}\right)^2 + Z''^2 = \frac{R^2}{4}\right]$ in the complex impedance plane that intersects the real axis at both the origin and R. Following is an expression that describes the impedance of a $R \parallel C$ combination.

$$\frac{1}{Z} = \frac{1}{R} + \frac{1}{(1/i\omega C)} \quad \ldots\ldots (3.11)$$

$$\therefore Z = \frac{R}{1 + i\omega RC} = \frac{R}{1 + (\omega RC)^2} - i\frac{\omega R^2 C}{1 + (\omega RC)^2} \quad \ldots\ldots (3.12)$$

$$where, \quad Z' = \frac{R}{1 + (\omega RC)^2} \quad \ldots\ldots (3.13) \quad and\ Z'' = -\frac{\omega R^2 C}{1 + (\omega RC)^2} \quad \ldots\ldots (3.14)$$

$$\therefore \frac{Z''}{Z'} = \omega(RC) \quad \ldots\ldots (3.15)$$

Using Eq. (3.14) and (3.15), Eq. (3.13) can be rewritten as…

$$Z' = \frac{R}{1 + \left(\frac{Z''}{Z'}\right)^2}$$

$$\therefore Z'^2 - RZ' + Z''^2 = 0$$

and therefore, $$\left(Z' - \frac{R}{2}\right)^2 + Z''^2 = \frac{R^2}{4} \quad \ldots\ldots (3.16)$$

Eq. 3.16 is the equation of a circle with a radius of $\frac{R}{2}$ and a centre at $\left(\frac{R}{2}, 0\right)$.Therefore, the Z'' vs. Z' (Nyquist) plot confirms a semicircle with a radius of $R/2$ and $\tau = RC = 1/\omega_{max}$ as time constant.

The Nyquist diagram is a graphical representation of impedance or admittance data and is commonly used in electrochemical impedance spectroscopy (EIS) measurements. In such situations, the presence of blocking electrodes can cause a semicircle with a spike to appear in the Nyquist diagram. To account for this behaviour in an equivalent circuit, a parallel combination of a resistor (R) and a capacitor (C) is placed in series with the blocking electrode. The straight line in the diagram represents the capacitive behaviour of the electrode-electrolyte polarization, while $R \parallel C$ is related to the bulk property Fig. 3.10(e). In most of the research publications [1]–[4], a depressed half-circle with a tilted spike is observed in the Nyquist diagram due to the presence of a Constant Phase Element (CPE), which represents a leaky capacitor. The center of the circle in this case is shifted below the real axis.

The impedance response is characterized by a depressed semicircle in the complex plane, with parameters such as resistance (R) and leaky capacitive element (CPE) determined by the microscopic properties of the material. Furthermore, it appears that the origin of the depressed semicircle is due to polarization effects at the interface between blocking electrodes and the glass, resulting in a geometric capacitor (C) and a leaky capacitive element (CPE). The angle of depression and the inclination angle of the semicircle are also determined by microscopic properties. Overall, the impedance response of the circuit or real solid electrolyte would be a depressed arc below the real axis, intersecting at R and 0 (the origin), and forming an angle of $\alpha\pi/2$, depicted in Fig. 3.10(f).

In the present investigation, complex impedance measurements were carried out to determine the electrical conductivity and the AC behaviour of the borophosphate glasses doped with metal halides of lithium, sodium, and silver over a range of temperatures and frequencies.

***Figure 3.11**: Solartron-1260A-Frequency Response Analyzer.*

The Solartron 1260A impedance Analyser was used to carry out the impedance measurements in a frequency range of $1\,Hz$ to $32\,MHz$ at various temperatures (Fig. 3.11). The silver-paste ion-blocking electrodes were applied on both sides of the glass sample to establish a regulated contact area for the ionic conductivity measurement. The sample was held at each temperature for 10 minutes to ensure thermal equilibrium.

(b) Complex Conductivity Formalism

In 1987, Ingram [5] analysed an alternating current (AC) response of electrolytes. For the first time, researchers led by Grant et al; [6] have measured the frequency-dependent conductivity of a glassy solid electrolyte that conducts silver ions. For the investigation purpose, the silver-containing compound glass system was chosen and found that it follows Jonscher power law behaviour for frequency- dependent bulk conductivity.

Following are the relation to calculate complex conductivity with the help of impedance data. $\sigma^{"}$ is known as AC conductivity. $\sigma^{"}$ has been extensively utilised, analysed, and interpreted by worldwide researchers [7], [8] to study and analyse multiple electrical properties of ion-conducting materials such as glasses, crystals, and polymers.

$$\sigma^{*} = \frac{t}{a}\left(\frac{Z' + iZ^{"}}{Z'^{2} + Z^{"2}}\right) \quad \ldots..(3.17), and\ \sigma^{*} = \sigma' + i\sigma^{"} \quad \ldots..(3.18)$$

$$\sigma' = \frac{t}{a}\left(\frac{Z'}{Z'^{2} + Z^{"2}}\right) \quad \ldots..(3.19), and\ \sigma'' = \frac{t}{a}\left(\frac{Z^{"}}{Z'^{2} + Z^{"2}}\right) \quad \ldots..(3.20)$$

In glass-like disordered systems, AC conductivity spectra provide valuable information about the relaxation mechanism of the material. The conductivity spectra typically exhibit a frequency-dependent behaviour, where the conductivity increases with increasing

frequency until it reaches a plateau at low frequencies. This plateau corresponds to the DC conductivity of the material, which arises from the long-range translational hopping of ions. At higher frequencies, the conductivity transitions from the frequency-independent plateau region to a frequency-dependent region. This transition marks the onset of the relaxation behaviour of the ions in the material. The relaxation process is characterized by short-distance back-and-forth hopping between equivalent sites, which results in a frequency-dependent conductivity response. This behaviour is often referred to as dispersion. The AC conductivity spectra can provide insights into the different hopping mechanisms and the distribution of relaxation times in the material. By analyzing the shape and frequency dependence of the spectra, one can gain a better understanding of the material's physical properties and design more effective electrolytes for energy storage and conversion applications.

The illustration depicts in Fig. 3.12, is the typical AC conductivity spectra for the Ag^+ ion conducting $AgI - Ag_2O - B_2O_3$ glass system [9]. The extrapolation of the plateau of the low-frequency region helps to derive the sigma dc value before the high-frequency dispersion region. As one can see from the Fig. 3.12, the well-known universal Jonscher Power Law (JPL) is the best fit for the frequency-dependent conductivity spectrum of the silver ion conducting system [10].

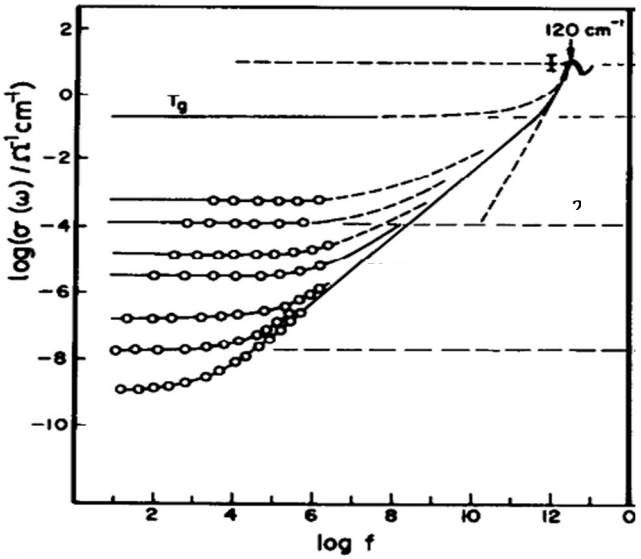

***Figure 3.12**: Frequency dependent conductivity of $AgI - Ag_2O - B_2O_3$ fast ion conduction system.*

$$\sigma'(\omega) = \sigma_0 + A\omega^n \quad \ldots\ldots (3.21)$$

Where, $\sigma'(\omega)$ is the real part of frequency (radial) dependent conductivity, σ_0 is the bulk conductivity or say DC conductivity σ_{dc}, arbitrary constant A determines the magnitude of dispersion at high frequency and n is the power law exponent/frequency exponent having value $0 < n < 1$. In Eq. 3.21, the first term σ_0 corresponds to DC or frequency-independent part, and the second part is of Constant Phase Element type.

The Eq. 3.21 can be rewritten by making use of Jonscher's empirical equation as,

$$\sigma'(\omega) = K\omega_p + K\omega_p^{1-n}\omega^n \quad \ldots\ldots (3.22)$$

Where, ω_p is the hopping frequency and K is mobile ion/charge carrier concentration.

After the theories given by Debye, Onsager, and Faulkenhagen about the frequency dependence of conductivity, Jonscher's theory of dielectric relaxation explains the frequency dependence of conductivity in terms of the dynamics of the ionic environment. According to this theory, when a charged carrier moves through a material, it causes a local distortion in the lattice potential energy that affects the motion of other charges in the vicinity. This distortion creates an "effective potential energy" landscape that is different from the true minimum energy landscape of the lattice. As a result, when an ion hops to a new site with a minimum lattice potential energy, it is still displaced from the true minimum potential energy, which includes the contribution of other mobile defects. This displacement creates an electric dipole moment that interacts with the local electric field, contributing to the conductivity of the material. However, this dipole moment is not static, but rather it fluctuates with time due to the movement of other charges in the material. These fluctuations result in a time-dependent conductivity that varies with frequency. At shorter timescales, the conductivity is limited by the frequency-dependent relaxation of the defect cloud around the charge carrier. As time goes on, this relaxation process reduces the frequency-limiting conductivities, leading to a power law-CPE (constant phase element) behavior zone in between.

(c) Complex Dielectric Formalism

Dipolar relaxation in materials consisting of permanent dipoles, causes re-orientation and results in the frequency-dependent feature of complex permittivity. Ion conduction and ion polarisation are integrated (inseparable) as a single process in an ion-conducting system.

Glasses are a type of ion-conducting material that can exhibit electronic, ionic, and space charge contributions to their electrical conductivity. The permittivity of glasses, which is a measure of their ability to store electrical energy in an electric field, is typically less than 20. When an electric field is applied to an ion-conducting material such as glass, mobile ions can move and accumulate at the sample-electrode interface, causing polarization in the material. This polarization can be described by the complex dielectric formalism, which takes into account the contributions of dipoles, mobile ions, and other factors to the dielectric constant of the material.

Given below is the complex dielectric function (Eq. 3.23).

$$\varepsilon^*(\omega) = \frac{\sigma^*(\omega)}{i\omega\varepsilon_0} = \varepsilon' - i\varepsilon^{"} \quad \ldots\ldots(3.23)$$

where, ε_0 is the permittivity of free space and ω is the radial frequency. The dielectric constant and loss are the real and imaginary parts of $\varepsilon^*(\omega)$, and the expressions are as follows.

$$\varepsilon' = \frac{-1}{\omega C_0}\left(\frac{Z^{"}}{Z'^2 + Z^{"2}}\right) \quad \ldots\ldots(3.24), and \;\; \varepsilon'' = \frac{-1}{\omega C_0}\left(\frac{Z'}{Z'^2 + Z^{"2}}\right) \quad \ldots\ldots(3.25)$$

The spectra of a perfect Debye system include a sharp transition between low and high frequencies, with two plateau regions, ε_s (static dielectric constant/ static permittivity) and ε_∞ (high frequency permittivity) respectively, at either end of the spectrum (Fig. 3.13). $\Delta\varepsilon$ is the difference between them, which stands for dielectric relaxation strength, and the relaxation of hopping ions which induces it.

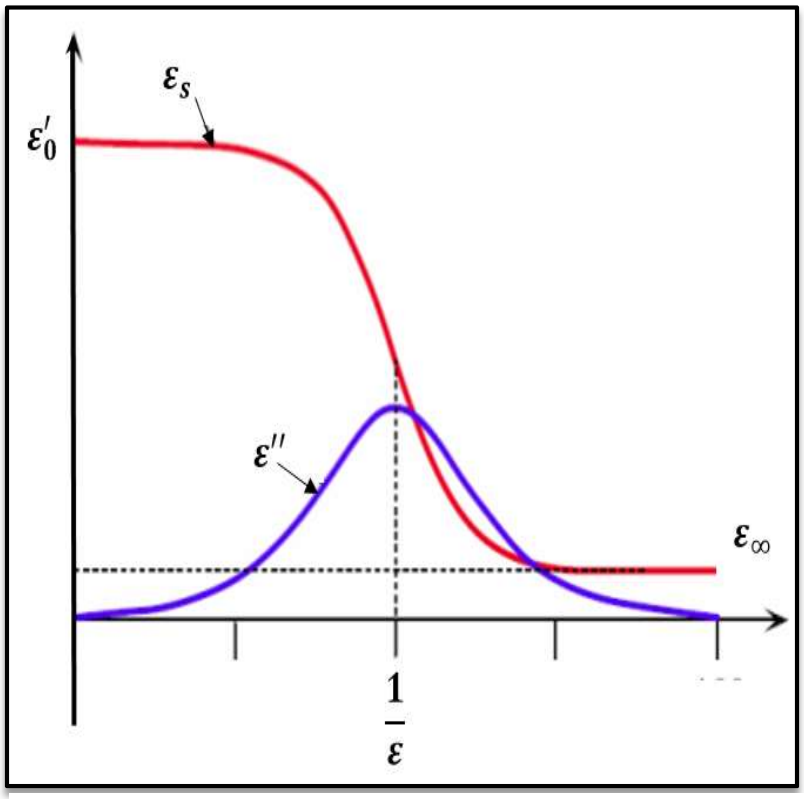

***Figure 3.13**: The relative permittivity is a complex number with real and imaginary part.*

$$\Delta\varepsilon = \varepsilon_s - \varepsilon_\infty \quad \ldots\ldots(3.26)$$

The calculation of ε_∞ is possible at a sufficiently high-frequency regime. But the determination of ε_s at low frequency is problematic because the dominant polarisation effect causes the accumulation of mobile ions at the electrode. So, it is hard to separate the true static dielectric constant from this polarisation effect.

The dielectric responses observed from a variety of materials demonstrate dispersion and distribution of relaxation durations that are primarily driven by hooping charge carriers, and they show deviation from ideal Debye behaviour.

The universal dielectric response, expressed as $\tan\delta$, demonstrates variation from the ideal Debye nature, that measures the ratio of electrical energy lost to the energy stored in periodic field having the value is equal to $\omega\tau$.

$$\tan\delta = \frac{loss\ factor}{permittivity} = \frac{\varepsilon^{"}}{\varepsilon'} = Constant \quad \ldots..(3.27)\ (Debye\ nature)$$

(d) Complex (Electric) Modulus Formalism

As a result of electrode polarisation and charge carrier transmission, the dielectric constant is relatively high at lower frequencies. Therefore, at the same instant, it is challenging to distinguish between the interfacial polarisation and the relaxing process. In the 1970s, Macedo formulated a new formalism to rectify the lower frequency issue, termed "dielectric modulus", also known as the electric or modulus function [11], [12].

The dielectric modulus is a complex function of frequency that characterizes the response of a material to an applied electric field. It is defined as the ratio of the complex permittivity to the complex modulus of a material, which provides a more direct measure of the relaxation process, without being affected by electrode polarization. The dielectric modulus has two components, the real part and the imaginary part, which are related to the elastic and dissipative responses of the material, respectively.

The real part of the dielectric modulus is related to the storage or elastic modulus, which represents the energy stored in the material during deformation. The imaginary part of the dielectric modulus is related to the loss or viscous modulus, which represents the energy dissipated as heat during deformation.

The complex electric modulus (M^*) is used to study the phenomenon of conductivity relaxation. It reduces the effects of polarisation caused by contact or interfaces (the Maxwell-Wagner effect), which gives a clearer picture of electrical relaxation process. The impedance spectroscopy data helps to estimate the complex modulus formalism (M^*), which is the reciprocal of complex dielectric permittivity.

The mathematical relation between dielectric modulus and dielectric permittivity is written as,

$$M^* = M' + i\,M^{"} \quad \ldots..(3.28)$$

$$M^* = \frac{1}{\varepsilon^*} = \frac{\varepsilon'}{\varepsilon'^2 + \varepsilon^{"2}} + i\frac{\varepsilon^{"}}{\varepsilon'^2 + \varepsilon^{"2}} \quad \ldots..(3.29)$$

where, $M'and\ M''$ are the real and imaginary part of electric modulus function.

The dielectric constant can be written in form of frequency independent permittivity and the DC conductivity as,

$$\varepsilon^* = \varepsilon_s - \frac{i\sigma_{dc}}{\omega\varepsilon_0} \quad \ldots\ldots(3.30)$$

$$= \varepsilon_s - \frac{i\varepsilon_s}{\omega\tau_\sigma}\left(\because \sigma_{dc} = \frac{\varepsilon_0\varepsilon_s}{\tau_\sigma} \& \tau_\sigma = \frac{\varepsilon_0\varepsilon_s}{\sigma_{dc}}\right) \quad \ldots\ldots(3.31)$$

By combining the Eq. (3.29) and (3.31) ofM^* and ε^*, the equation for M^* can be rewritten as follows,

$$\therefore M^* = M_s\left[\frac{i\omega\tau_\sigma}{1 + i\omega\tau_\sigma}\right]$$

$$M^* = M_s\left[\frac{(\omega\tau_\sigma)^2 + i(\omega\tau_\sigma)}{1 + (\omega\tau_\sigma)^2}\right]$$

$$= M' + i\,M''$$

where, τ_σ has the unit of time and known as conductivity relaxation time.

The Fig. 3.14 depicts real and imaginary parts of modulus against frequency for a glassy electrolyte. At lower frequencies, M' shows a tail-like curve approaching zero, and towards higher frequencies showing a step-like increase. The electrode polarisation makes a negligible contribution to M^*, while the dispersion is primarily due to conductivity relaxation.

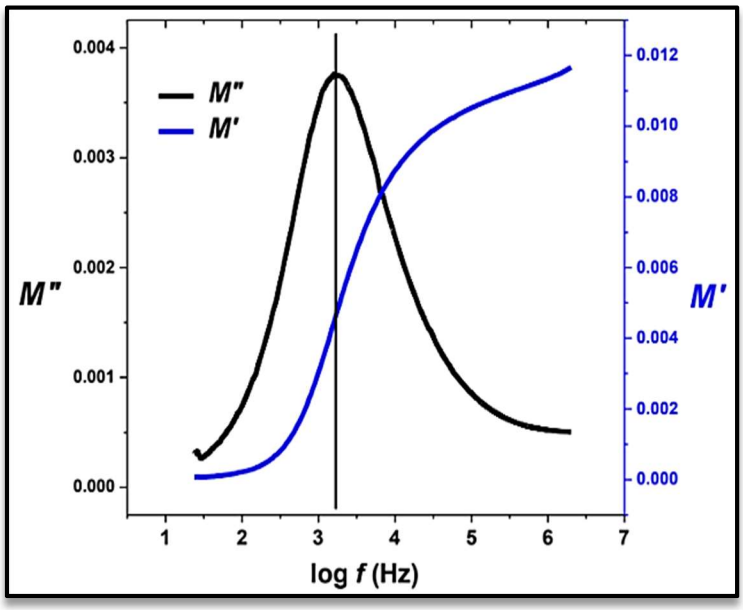

***Figure 3.14**: Electrical modulus against log f plot (real and imaginary part of modulus function)*

The capacitance associated with electrodes causes the M'' curve tail at lower frequencies. In the middle-frequency range, the M'' curve has broad and asymmetric distribution on both sides of the peak (maxima), exhibiting the non-Debye behaviour having multiple relaxation times. The long-range mobility of charge carriers, which contributes to dc conductivity, is a function of the frequency range below (left of the curve) the frequency of ω_C.

While higher side of the ω_c (right of the curve) of the spectrum, charge carriers are confined to their potential well and hop for short range span.

The frequency ω_c or ω_{max} at which the maximum M" occurs is often referred to as the "characteristic frequency" or "relaxation frequency" and it is given by,

$$\omega_c \tau_c = 1 \quad \ldots\ldots (3.32)$$

This frequency marks the transition from short-range to long-range mobility of charge carriers with frequency, as you mentioned. At frequencies below ω_c, the charge carriers have enough energy to move relatively long distances and contribute to dc conductivity. This is because they are not confined to their potential wells and can move freely within the material. On the other hand, at frequencies above ω_c, the charge carriers are confined to their potential wells and can only hop short distances. As a result, the conductivity decreases rapidly with increasing frequency.

The non-Debye behaviour of the $M^{"}$ curve in the middle-frequency range, with its broad and asymmetric distribution on both sides of the peak, indicates that the material has multiple relaxation times. This means that different types of charge carriers are present in the material, and each type has a different mobility and relaxation time.

The cause of the widened spectra of the $M^{"}$ versus $\log f$ curve is the relaxation time distribution for distinct processes. According to Hasz [13], the distribution of relaxation time is related to the distribution of free energy barriers for ionic jumps, wherein the distribution grows as the disorderliness increases. In contrast, Grant [6] has ascribed that the dispersion of relaxation periods not associated with the disordered structure of glasses but to the cooperative character of the conduction process analogous to the associated backwards-forward hopping of ions.

The Kohlrausch-William-Watts (KWW) function is a mathematical function used to describe the relaxation behavior of materials under an external stimulus, such as an electric field. The KWW function is given by:

$$M"(\omega) = M^{"}_{max}\, exp[-(i\omega\tau)^{\beta}]$$

Where, $M^{"}(\omega)$ is the imaginary part of the complex modulus, $M^{"}_{max}$ is the maximum value of $M^{"}(\omega)$, τ is the characteristic relaxation time, ω is the angular frequency, and β is a stretching exponent that determines the degree of non-exponential behavior. The KWW function is particularly useful in describing the relaxation behaviour of materials that exhibit a stretched exponential decay, where the relaxation time distribution is broad and the decay

is slower than a single exponential [14]. The function $\varphi(t)$ mentioned in the statement is related to the KWW function and describes the time-dependent behaviour of the material's response to the external stimulus. Specifically, $\varphi(t)$ is given by:

$$\varphi(t) = (1/\tau)\beta\, t^{(1-\beta)}\, exp[-(t/\tau)\beta]$$

This function has a maximum value at $t = 0$ and then decays with time in a non-exponential manner, reflecting the stretched potential character of electric field relaxation.

$$\varphi(t) = \varphi_0 \exp\left(\frac{-t}{\tau}\right)^{\beta} \quad \ldots..(3.33)$$

$$\beta = \left(\frac{1.14}{FWHM}\right) \quad \ldots..(3.34)$$

where, β is the stretched/ relaxation/ Kohlrausch parameter $(0 < \beta < 1)$, and τ is the characteristic relaxation time.

The width at half height of the $M^{"}/M^{"}_{max}$ plot leads to the stretched parameter. The value of the Kohlrausch parameter (β) for most of the solid electrolytes is less than one. The greater deviation of Debye-relaxation is caused due to smaller the value of β. It was hypothesised by Hodge et al; [15] that the value of β is a signpost for the presence of ionic conduction in glasses.

The concept of coordinated motion in glasses is a key aspect of Jonscher's universal behaviour. In glasses, the motion of charged particles, such as ions, is not independent or isolated, but rather involves a coordinated relaxation of the applied field. This coordinated motion leads to a reduction in the β value, which characterizes the frequency dependence of the complex permittivity of a material.

When an ion hops from one equilibrium position to another in the vicinity, it causes a perturbation in the surrounding charges, which in turn results in further relaxation of the applied field. This coordinated motion between the charges is a complex process that involves many interacting factors, including the structure and dynamics of the glass, the properties of the charges themselves, and the nature of the applied field.

The reduction in the β value is a consequence of this coordinated motion, which tends to reduce the frequency dependence of the complex permittivity. This effect is observed across a wide range of glassy materials and is an important aspect of their behaviour.

Jonscher's universal behaviour provides a framework for understanding this coordinated motion and its relationship to the frequency dependence of the complex permittivity in glasses.

If one knows the conductivity relaxation time (τ_σ) and glass transition temperature (T_g), which is the ability of the mobile ions to move around in the glass, then one can find glass decoupling index R_τ, which measures how well the motion of conductive ions can detach/decouple from the glassy material.

$$R_\tau = \frac{\tau_s}{\tau_\sigma} \quad \ldots\ldots (3.35)$$

The calculation of structural relaxation (τ_s)is complicated for various temperatures except for the glass transition temperature.

However, the determination of τ_σ (T_g) values is by extrapolating the $\log \tau_\sigma$ against $1000/T$ plot to the T_g value of the respective sample and it is assumed that the structural relaxation period τ_s is $200s$ at T_g.

$$R_\tau = \frac{200}{\tau_\sigma} \quad \ldots\ldots (3.36)$$

The value of R_τ which is system dependent and varies between 10^{-14} and 10^{-13}.

Macedo [11], [12] says that the short Maxwell time parameter, $\langle \tau_\sigma \rangle$, which is also known as the mean of the distribution of relaxation time, is the most practical way to calculate DC conductivity.

$$\langle \tau_\sigma \rangle = \frac{\varepsilon_0 \varepsilon_\infty}{\sigma_{dc}} = \frac{9 \times 10^{-13}}{\sigma_{dc}} \quad \ldots\ldots (3.37)$$

Macedo and associates [12] have expressed the following example of an average relaxation time distribution.

By integrating the mathematical relationships of the distributed relaxation time with the decoupling index Eq. 3.36 and DC conductivity Eq. 3.37, the equation is as follows.

$$R_\tau = \frac{200}{9 \times 10^{-13}} \sigma_{dc} \quad \ldots\ldots (3.38)$$

$$\therefore \log R_\tau = 14.3 + \log \sigma_{dc} \quad \ldots\ldots (3.39)$$

Using the extrapolation of Arrhenius plots of conductivity from Eq. (3.38) and (3.39), the σ_{dc} value at the glass transition temperature is estimated.

Bibliography

[1] V. A. Adhwaryu and D. Kanchan, "Ionic transport studies in silver borophosphate glass system with silver iodide," *AIP Conf. Proc.*, vol. 2115, no. July, pp. 1–5, 2019, doi: 10.1063/1.5113107.

[2] M S Jayswal, "Transport Properties of PbI2 doped Silver Oxysalt based Amorphous Solid Electrolytes," The M S University of Baroda, Vadodara, Vadodara, 2014.

[3] A. R. Kulkarni, H. S. Maiti, and A. Paul, "Fast ion conducting lithium glasses-Review," *Bull. Mater. Sci.*, vol. 6, no. 2, pp. 201–221, 1984, doi: 10.1007/BF02743897.

[4] C. Calahoo and L. Wondraczek, "Ionic glasses: Structure, properties and classification," *J. Non-Crystalline Solids X*, vol. 8, p. 100054, 2020, doi: 10.1016/j.nocx.2020.100054.

[5] M. D. Ingram, "Ionic Conductivity in Glass," *Phys. Chem. Glas.*, pp. 214–234, 1987.

[6] R. J. Grant, M. D. Ingram, L. D. S. Turner, and C. A. Vincent, "Optimized ionic conductivity in glass. Vitreous silver arsenate iodide (Ag7I4AsO4) electrolytes," *J. Phys. Chem.*, vol. 82, no. 26, pp. 2838–2844, Dec. 1978, doi: 10.1021/j100515a019.

[7] A. K. Jonscher, "A new understanding of the dielectric relaxation of solids," *J. Mater. Sci.*, vol. 16, no. 8, pp. 2037–2060, Aug. 1981, doi: 10.1007/BF00542364.

[8] S. H. Chung, K. R. Jeffrey, J. R. Stevens, and L. Börjesson, "Dynamics of silver ions in (AgI)x-(Ag2O-nB2O3)1-x glasses: A Ag109 nuclear magnetic resonance study," *Phys. Rev. B*, vol. 41, no. 10, pp. 6154–6164, 1990, doi: 10.1103/PhysRevB.41.6154.

[9] C. A. Angell, "Correlation of mechanical and electrical relaxation phenomena in superionic conducting glasses," *Mater. Chem. Phys.*, vol. 23, no. 1–2, pp. 143–169, Aug. 1989, doi: 10.1016/0254-0584(89)90022-9.

[10] A. K. Jonscher, "The 'universal' dielectric response," *Nature*, vol. 267, no. 5613, pp. 673–679, Jun. 1977, doi: 10.1038/267673a0.

[11] F. S. Howell, R. A. Bose, P. B. Macedo, and C. T. Moynihan, "Electrical Relaxation in a Glass-Forming Molten Salt."

[12] P. B. Macedo, C. T. Moynihan, and R. Bose, "No Title," *Phys. Chem. Glas.*, vol. 13, no. 171, 1972.

[13] W. . Hasz, C. . Moynihan, and P. . Tick, "Electrical relaxation in a CdF2LiFAlF3PbF2 glass and melt," *J. Non. Cryst. Solids*, vol. 172–174, pp. 1363–1372, Sep. 1994, doi: 10.1016/0022-3093(94)90664-5.

[14] C. T. Moynihan, L. P. Boesch, and N. L. Laberge, "Decay function for the electric field relaxation in vitreous ionic conductors", *Phys. Chem. Glas.* , vol. 14, pp. 122–125, 1973.

[15] I. M. Hodge, K. L. Ngai, and C. T. Moynihan, "Comments on the electric modulus function," *J. Non. Cryst. Solids*, vol. 351, no. 2, pp. 104–115, Jan. 2005, doi: 10.1016/j.jnoncrysol.2004.07.089.